JOURNAL OF combinatorial CHEMISTRY

Article

Solid-Phase Synthesis of Tetrasubstituted Pyrazoles, Novel Ligands for the Estrogen Receptor

Shaun R. Stauffer, and John A. Katzenellenbogen

J. Comb. Chem., **2000**, 2 (4), 318-329• DOI: 10.1021/cc0000040 • Publication Date (Web): 18 May 2000

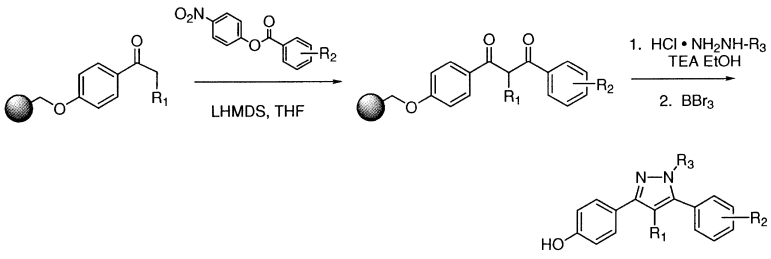

More About This Article

Additional resources and features associated with this article are available within the HTML version:

- Supporting Information
- Links to the 2 articles that cite this article, as of the time of this article download
- Access to high resolution figures
- Links to articles and content related to this article
- Copyright permission to reproduce figures and/or text from this article

View the Full Text HTML

Journal of Combinatorial Chemistry is published by the American Chemical Society.
1155 Sixteenth Street N.W., Washington, DC 20036

Solid-Phase Synthesis of Tetrasubstituted Pyrazoles, Novel Ligands for the Estrogen Receptor

Shaun R. Stauffer and John A. Katzenellenbogen*

Department of Chemistry, University of Illinois, Urbana, Illinois 61801

Received January 11, 2000

Most ligands for the estrogen receptor (ER) are not well suited for synthesis by combinatorial means, because their construction involves a series of carbon−carbon bond forming reactions that are not uniformly high yielding. In previous work directed to overcoming this limitation, we surveyed various phenol-substituted five-membered heterocycles, hoping to find a system that would afford both high ER binding affinity and whose synthesis could be adapted to solid-phase methods (Fink et al. *Chem. Biol.* **1999**, *6*, 206−219.) In this report, we have developed a reliable and efficient solid-phase method to prepare the best of these heterocycles, the tetrasubstituted pyrazoles, and we have used this methodology to produce small, discrete libraries of these novel ER ligands. We used a combination of FT-IR and nanoprobe ^{1}H NMR-MAS to characterize intermediates leading up to the final pyrazole products directly on the bead. We also developed a scavenging resin, which enabled us to obtain products free from inorganic contaminants. We prepared a 12-member test library, and then a 96-member library, and in both cases we determined product purity and ER binding affinity of all of the library members. Several interesting binding affinity patterns have emerged from these studies, and they have provided us with new directions for further exploration, which has led to pyrazoles having high affinity and potency as agonists and antagonists toward the ERα subtype.

Introduction

In recent years, combinatorial chemistry, with its ability to generate a large set of structurally related analogues, has become a bona fide tool for increasing productivity in the functional assessment of compound libraries and the rapid development of structure−activity relationships.[1] Combinatorial techniques for preparing peptide libraries are well established, but methods for the combinatorial synthesis of small-molecule libraries for the development of useful pharmaceuticals remains a formidable challenge. Small molecules are generally not oligomeric, and a diverse range of chemical transformations may be required for their synthesis. Therefore, the development of an appropriate parallel synthesis format is not always straightforward. This limitation is increasingly encountered in the quest for chemical diversity, because the fidelity of a given library member can be compromised when the building block components are not uniformly reactive. Consequently, there has been an active quest to develop the sort of truly general, high yielding transformations necessary to maintain high quality in the preparation of small-molecule libraries.

Novel estrogens having tissue selective action suitable for menopausal hormone replacement or the treatment and prevention of breast cancer are actively being sought by the pharmaceutical industry.[2] These agents, often referred to as selective estrogen receptor modifiers or SERMs, generally consist of a nonsteroidal core structure onto which is appended a basic or polar function.[3] Most ligands for the estrogen receptor (ER), however, are not well suited for synthesis by combinatorial means, because their construction generally involves a series of carbon−carbon bond forming reactions that are not uniformly high yielding, nor necessarily easily adaptable to solid-phase synthesis methods. Two small combinatorial libraries of nonsteroidal ER ligands have been reported,[4,5] but these efforts produced either low affinity ligands or ones of limited structural diversity.

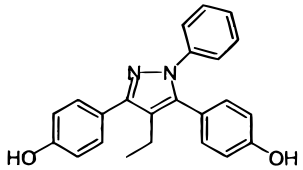

1 RBA = 14 %

Figure 1. Estrogen receptor-α selective pyrazole discovered from a solution-phase study. RBA is relative binding affinity for the estrogen receptor; for estradiol, RBA = 100%.

To circumvent these current limitations and to expand the possible combinatorial approaches to ER ligands, we have proposed a novel modular ER pharmacophore consisting of a *variable* core structure, onto which are linked four independent substituents of defined variability. Using this paradigm, we have investigated core structures consisting of five-membered heterocycles, as well as other functionalities.[6] Among the five-membered systems that we have studied to date, we found that 1,3,5-triaryl-4-alkyl-pyrazoles, such as compound **1** (Figure 1), showed high binding affinity for the estrogen receptor, and intriguingly this compound had 100-fold higher potency as an agonist in a cell-based transcription assay through ERα than through ERβ.[7] Com-

* Address correspondence to: John A. Katzenellenbogen, Department of Chemistry, University of Illinois, 600 South Mathews Avenue, Urbana, Illinois 61801; 217 333 6310 (phone); 217 333 7325 (fax); jkatzene@uiuc.edu (e-mail).

10.1021/cc0000040 CCC: $19.00
Published on Web 05/18/2000

Scheme 1. Routes for the Preparation of the 12-Member and the 96-Member Pyrazole Libraries

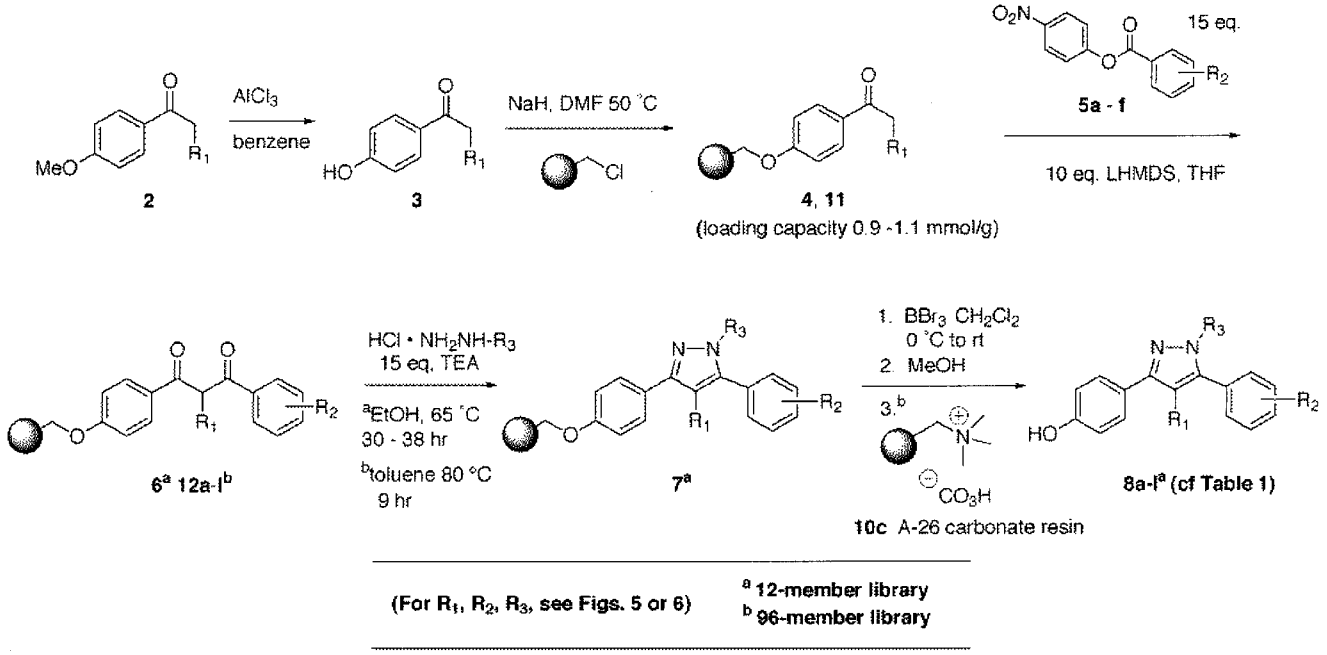

pounds that show high ER subtype selectivity are in great demand as agents to define the biological roles of these subtypes[8] and as potential tissue-selective estrogens for the uses noted above.

Because of these interesting initial findings, we wished to use a combinatorial approach to explore this pyrazole template further, to gain a better understanding of its structure−binding affinity pattern with the ER and to discover additional compounds with ER subtype selectivity. In particular, we hoped that such an expanded study would enable us to determine the preferred binding orientation for these pyrazoles in the ER, an issue that was not settled by our initial investigations.[6] We required this information to guide our future placement of pharmacophore elements in the design of selective antiestrogens (Stauffer, S. R., Huang, Y., Aron, Z., Coletta, C. J., Sun, J., Katzenellenbogen, B. S., Katzenellenbogen, J. A., unpublished).

As we had noted in their original conception,[6] the tetrasubstituted pyrazoles offer an attractive template for the combinatorial development of ligands for the estrogen receptor. Their heterocyclic nucleus provides a core upon which several common substructural motifs found in high affinity ER ligands can adequately be displayed in several possible configurations, and their synthesis involves simple condensation reactions, some of which have already been demonstrated on solid phase, although mostly for trisubstituted pyrazole derivatives.[9−12]

This work describes our efforts in the design and preparation of libraries of tetrasubstituted pyrazoles as ER ligands and our evaluation of the binding affinities of the library members. These studies have led us to a new series of high affinity compounds that display very high ERα agonist selectivity in cell-based transactivation assays, the details of which will be reported elsewhere (Stauffer, S. R., Sun, J., Katzenellenbogen, B. S., Coletta, C. J., Katzenellenbogen, J. A., unpublished).

Results and Discussion

Library Strategy. It was our intention to prepare discrete analogues (96-member libraries) of our tetrasubstituted pyrazole pharmacophore, noted above, in a parallel split-split format to produce material for ER binding affinity assays. Synthetically, the classical 1,3-dione-hydrazine condensation route (illustrated in Scheme 1) seemed attractive, because it is well precedented and can be accomplished under conditions that are potentially adaptable to solid-phase synthesis.[6] Also, the β-diketone component can be readily generated from a crossed-Claisen condensation reaction.

Using this route, we can introduce molecular diversity in the target pyrazole in either the alkylphenone, the ester, or the hydrazine component. Our choice to introduce the C-4 alkyl group early on within the ketone, rather than by alkylating the β-diketone intermediate, was based on solution feasibility studies; in contrast to the pyrazole synthesis strategy reported by Marzinzik and Felder,[9] we found that alkylation was not general for the preparation of 1,3-diarylpropane-1,3-diones. Our approach is also attractive because many of the 4′-methoxy-alkylphenone precursors are commercially available or can be produced in one step via Friedel−Crafts acylation reactions.

Linker. We selected the phenol component as the site for attachment of the pyrazole to the polymer support because it is convenient and it is the one functional group that is present in all of the pyrazoles. Merrifield's resin was used as the solid support, so the tethered phenol became attached to the resin as a *p*-substituted benzyl ether.

Our overall linker strategy is advantageous for two reasons: First, we knew from solution studies for tetrasubstituted pyrazoles of this type that a robust linker would be required to withstand the conditions for pyrazole formation (DMF/THF 120 °C).[6] Thus, we expected that the stable benzyl ether link would be more satisfactory than other more labile linkers. Second, we anticipated that the strong acidic

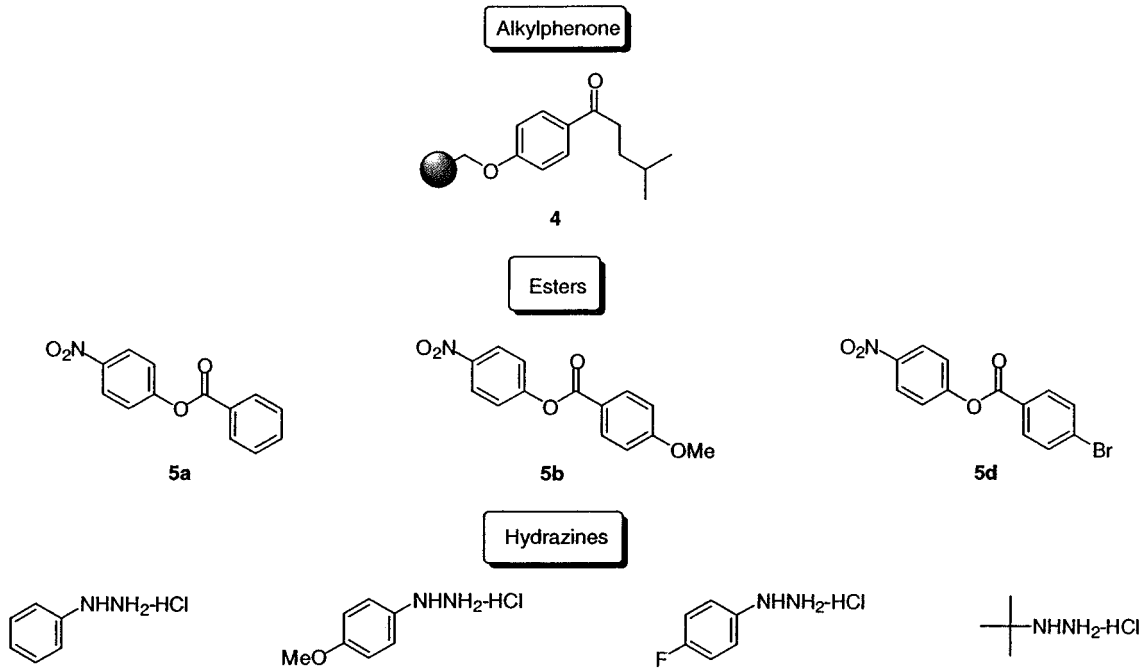

Figure 2. Components for 12-member library.

conditions required for product cleavage from the resin (i.e., BBr_3) could be adjusted to cleave, as well, any methyl ethers protecting other phenolic components. This approach is similar to that reported by Green for the preparation of lavendustin analogues,[13] but different in that our linker is a benzyl ether rather than a benzyl ester.

Method Development. The adaptation of the pyrazole synthesis from solution phase to solid phase required extensive optimization and later modification. Our initial route is shown in Scheme 1, and it was used for the preparation a small 12-member library, which was intended to serve as a standard for later, larger library design. In addition, this smaller library was developed to evaluate the generality of the reaction conditions by using various electronically demanding building blocks (Figure 2). The conditions described below were initially developed using our original lead compound **1** as a model.

Few starting alkylphenones (**2**, Scheme 1) are available commercially, but they were readily prepared via Friedel−Crafts acylation, using anisole and the desired acid chloride. Thus, the protected *p*-methoxy-alkylphenone **2** was obtained and then demethylated using $AlCl_3$ to afford **3**, which was subsequently loaded onto Merrifield's resin (Novabiochem Inc., 1.39 mmol/g), according to the method of Ellman and co-workers.[14] Formation of the resin-bound ketone **4** was ascertained using standard techniques (FT-IR, null %Cl combustion analysis), and a portion was cleaved with BF_3−SMe_2 to determine the loading capacity based on mass recovery. After minimal workup, the expected ketone was cleanly observed by ^{1}H NMR and HPLC (purity >99%), and the loading capacity was found to be between 0.9 and 1.1 mmol/g.

Following ketone immobilization, we used a crossed-Claisen condensation reaction to form the requisite β-diketones (**6**). This transformation proceeds satisfactorily using excess lithium hexamethyldisilazide (LHMDS) and activated *p*-nitrophenyl esters (**5a**,**b**,**d**) in THF. Other bases, such as $NaNH_2$ or KO*t*-Bu, were less effective, particularly with higher alkylphenones (e.g., propiophenone and higher). In addition, *p*-nitrophenyl activated esters proved to be most general in providing high yields of the dione. In most cases, the active ester could be present in the reaction vessel during the addition of base. However, esters with electron withdrawing groups, such as compound **5d** (Figure 2), required preformation of the resin-bound enolate prior to the addition of the ester, because of competing nucleophilic addition of the disilamide anion to the activated ester.

We found nanoprobe ^{1}H NMR-MAS to be an indispensable tool for following β-dione formation on solid-phase and for optimizing reaction conditions. Although FT-IR was useful for monitoring ketone immobilization, we did not find it satisfactory for evaluating the progress of dione formation. We had expected that a shift in the C=O stretch of the alkylphenone at 1675 cm^{-1} would occur as the dione formed and equilibrated with its intramolecularly hydrogen bonded enol tautomer. We were surprised, however, when the ^{1}H NMR spectrum of 1,3-bis(4-methoxyphenyl)-2-ethyl-1,3-propanedione showed that these α-substituted β-diketones exist exclusively in the diketo tautomeric form in solution. We presume that this is due to the A-strain present in these substituted molecules, because ^{1}H NMR analysis shows that the less hindered 1,3-diaryl-1,3-propanediones, which do not bear a 2-alkyl substituent, exist as mixtures of both enol and diketo tautomers. In most cases FT-IR revealed a C=O doublet for the dione. However, the intensity of this signal was often weak and variable, and thus was not a reliable indicator of reaction progress. In contrast, by using ^{1}H NMR-MAS and nanoprobe technology, we were able to conveniently and quickly ascertain the level of β-diketone formation.

Shown in Figure 3 panel A (top) is the spectrum for the starting resin-bound 4-hydroxy-butryophenone, and in panel

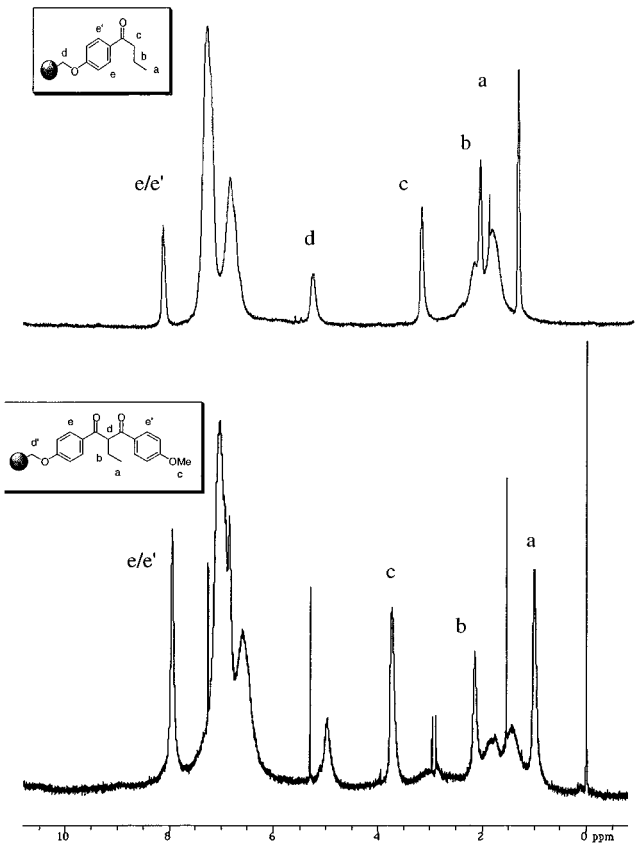

Figure 3. Panel A (top): ^{1}H NMR-MAS of polymer-bound butryophenone derivative **11**. Panel B (bottom): ^{1}H NMR-MAS of β-diketone product **12b** after Claisen condensation reaction.

B (bottom) is the spectrum for the expected dione product after Claisen condensation with 4-methoxy-(4′-nitrophenyl)-benzoate. Because we are using a short linker, which holds these molecular segments close to the rigid polystyrene backbone, the line widths for these signals remain fairly large (20 Hz), and as a result, coupling information is unavailable. Despite this limitation, however, we can readily discern diagnostic chemical shift differences between the product and starting material, so that we confidently assess the success or failure of the reaction.

To form the tetrasubstituted pyrazole on solid phase, we first tried conditions that had been successfully used for the solution-phase synthesis (heating the dione and hydrazine hydrochloride salt to 110−120 °C in DMF/THF solutions for up to 16 h), as well as conditions developed my Marzinzik and Felder for solid-phase pyrazole synthesis (DMA as a solvent at 80 °C).[9] Unfortunately, even with extended heating, neither of these methods gave the desired heterocycle. When we used triethylamine (TEA) to neutralize the hydrazine hydrochloride and DMF as solvent, we obtained low yields of the desired product, but purity after cleavage/deprotection was less than 35%. Ultimately, we found that toluene as solvent with the addition of TEA was effective, affording the pyrazole product **1** in >90% purity after cleavage/deprotection. One should note that subsequently we found that these reaction conditions, which involved heating toluene to 80 °C for 9 h, were not compatible with our 96-well reaction plate (Polyfiltronics 96-well Unifilter plate). Nevertheless, at the time we used these conditions to prepare a 12-member library of pyrazoles and then later modified the pyrazole-forming step to make it compatible with our 96-well reaction plate (see below).

Table 1. HPLC Purity Determination and Estrogen Receptor Binding Affinities (RBA Values) of C(4) *i*-Butyl Pyrazole Library

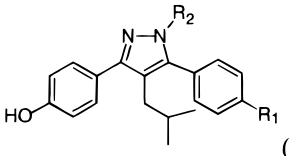

(**8a – l**)

compd	R_1	R_2	HPLC purity[a] (%)	% RBA[b]
8a	H	Ph	80	0.38/0.13[c]
8b	H	*p*-OHC_6H_4	67	9.3/0.86[c]
8c	H	*p*-FC_6H_4	92	0.04
8d	H	*t*-Bu	29	0.47
8e	OH	Ph	62	5.4
8f	OH	*p*-OHC_6H_4	>99	7.6
8g	OH	*p*-FC_6H_4	90	4.0
8h	OH	*t*-Bu	23	3.8
8i	Br	Ph	75	0.76/0.01[c]
8j	Br	*p*-OHC_6H_4	>85	3.3
8k	Br	*p*-FC_6H_4	>80	0.17
8l	Br	*t*-Bu	28	0.90

[a] RP-HPLC, 80% MeOH:H_2O, flow rate of 1.0 mL/min, detection at 254 nm (performed before purification by radial chromatography). [b] Relative Binding Affinity (RBA) values determined by a modification of our standard competitive binding assay using only three concentrations of ligand; all compounds tested were at >80% purity. [c] Independent assays performed on the two individual regioisomers.

The diones (**6**) needed for this (and the larger library) were prepared in a single batch, using a homemade reaction block capable of holding 16−20 mL sealed conical polypropylene tubes as reaction vessels. The block was rotated in an oven at 40 °C for 4 h, using a modified rotary evaporator motor. After washing the resins and drying them overnight, we verified dione formation by nanoprobe ^{1}H NMR-MAS. Each dione resin was then split into the appropriate number of portions and reacted with the appropriate hydrazine, the cyclization products then being cleaved/deprotected with BBr_3. For this smaller 12-member library, the cleaved material was collected, treated to a minimal workup (MeOH, passage through a SiO_2 plug), and analyzed for purity by HPLC.

Shown in Table 1 are the HPLC-evaluated purities and the ER binding affinities for the C-(4)-*iso*-butyl pyrazoles (**8a**−**l**) in the 12-membered library. The HPLC purity values listed were obtained on the pyrazoles after only minimal workup, yet some of these are quite high (>90%). The pyrazoles derived from *tert*-butylhydrazine were of the lowest quality. The major byproduct in those having lower purity was the corresponding β-diketone intermediate, and in some cases small amounts of the starting ketone. Prior to binding affinity determination, all compounds were purified by radial chromatography, so that their purities were at least 80%. The molecular ions of all purified pyrazoles in the C(4) *i*-butyl series were also verified by ES-MS.

The binding affinities of these pyrazoles were determined in a competitive radiometric binding assay (for details see Experimental Section), using [^{3}H]estradiol as tracer and lamb

uterine cytosol as a source of ER, and they are expressed as relative binding affinity values (RBA), with estradiol having an RBA of 100%. In the past, we have found that repeat determinations of binding affinities by this assay have a coefficient of variation of 0.3.

We were concerned that even small amounts of contaminants in the purified pyrazoles might be affecting the RBA determinations. To test this, we examined the effect of dihydroxyphenyl dione **9** on the affinity determination of pyrazole **1**. This dione (**9**) itself binds to the ER only very weakly (RBA = 0.012%), and when it was added to pyrazole **1** at 10, 20, and 30%, we noted no effect on the RBA value obtained for pyrazole **1**. Thus, we believe that the binding affinity values we have determined for all of these pyrazoles (Table 1) are valid.

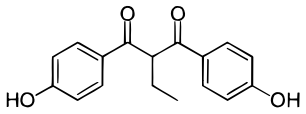

9 RBA = 0.012 %

Overall, the *i*-butyl pyrazoles bind to ER with reasonable affinity (Table 1), and even within this small set of compounds some structure−affinity trends are apparent. Clearly, there is a primary preference for hydroxy substitution at R_1, as in most cases, and the pyrazoles in the **8e**−**h** series bind better than those in the **8a**−**d** and **8i**−**l** series. Bromine substitution (series **8i**−**l**) is unusual for nonsteroidal ligands, but pyrazole **8j** (1.4:1 ratio of regioisomers) has a reasonable affinity of 3.3%. The reasonable affinity of the *tert*-butyl pyrazole **8h** suggests that bulky substituents other than phenyl are tolerated at R_2. The highest affinity members of this small pyrazole library, **8b** and **8f**, contain two and three hydroxyl substituents, respectively. The similar but lower affinity diphenolic pyrazole **8e** suggests that two distinct binding orientations may exist for **8e** and **8b**.

In those cases where more than one regioisomer was expected and they could be separated by HPLC, two RBA values are indicated. In three cases where we could do this, one regioisomer showed a higher affinity: In both the monohydroxy pyrazole **8a** and dihydroxy pyrazole **8b**, a 3−10-fold preference was found for one regioisomer, and in the case of pyrazole **8i**, this preference is much greater.

At this point, we could not make a definitive assignment of the structure of these regioisomers, but these results suggest that only one of them is providing an effective mimic of the A-ring of estradiol. In other work, we have carried out independent, regioselective syntheses of single pyrazole regioisomers in a related series, and we have conducted molecular graphics modeling studies of how these isomers might fit into the ligand binding domain of ER (Stauffer, S. R., Huang, Y., Coletta, C. J., Katzenellenbogen, J. A., unpublished). These studies suggest that there are indeed preferred orientations of these regioisomers within the ER binding pocket. However, it appears that the preferred orientation may switch, depending on the substituent display.

Adaptation to a 96-Well Format. To prepare the 96-member library, we used the Polyfiltronics 96-well Unifilter plate. The Unifilter plate contains a single underlying membrane which is designed to hold back most organic solvents, except when a vacuum is applied. Unfortunately, the Polyfiltronics plate did not withstand our conditions for pyrazole formation, using prolonged heating with toluene at 80 °C.

In our search for alternate conditions for pyrazole formation which the Polyfiltronics plate would withstand, we used pyrazole **1** as a model, and we explored a greater number of solvents and solvent mixtures for pyrazole formation (THF, BuCN, $HC(OMe)_3$, CH_3NO_2, and alcohols) with and without various additives ($TiCl_4$, Na_2SO_4, and 4 Å molecular sieves), at room temperature and at elevated temperatures. Ultimately, only alcohol solvents proved to be effective in forming the pyrazole product and were compatible with the Unifilter plate.

In this larger library, we also wanted to develop an expedited method for product isolation, whereby we could quench the cleavage/deprotection reagent BBr_3 and neutralize the HBr generated without introducing water, thereby avoiding cumbersome liquid−liquid phase extractions. Our approach was to develop a scavenger resin to neutralize the HBr and remove the inorganic contaminants by sequestration. Our initial efforts were based on work by Cardillo and coworkers,[15] involving the use of macroreticular carbonate resin as a reagent in the hydrolysis of alkyl halides.

Resin **10a** (Scheme 2), which is readily prepared from the chloride form of the ion exchange Amberlyst A-26 resin, was effective in quenching the BBr_3, but not surprisingly the final product was contaminated with NaBr. However, by modifying the resin to a sodium-free, bicarbonate form, we could still neutralize the HBr, but now with the liberation of only CO_2 and H_2O. Moreover, the polymer-bound quaternary ammonium groups sequestered any bromide ions from solution. Thus, by treating the crude cleaved/deprotected product with this bicarbonate resin, we could remove all of the inorganic contaminants, leaving the desired pyrazole remaining in solution together with only MeOH (bp 65 °C), $B(OMe)_3$ (bp 58 °C), and a small amount of H_2O, so that solvent removal gave the product free from any reagent contamination.

Two methods were used to prepare the bicarbonate form of A-26 resin (Scheme 2). Both resins (**10b** and **10c**) afford the product pyrazole in reasonable purity, but the bicarbonate resin which was prepared using $NaHCO_3$ (**10b**) still contained small amounts of Na ions, risking product contamination with NaBr. The preferred method to prepare Na ion-free resin was first to convert the chloride form of the A-26 resin to the hydroxide form and then generate the bicarbonate resin by bubbling CO_2 through an aqueous suspension of the resin. This ensured that there was no Na ion contamination, and this material (**10c**) afforded the pyrazole product with somewhat better purity. Shown in Scheme 1 is the overall optimized solid-phase synthesis route to the 96-member pyrazole library. The notable modifications from the original route used to prepare the 12-member library are the conditions for the pyrazole-forming step and final workup procedure involving the bicarbonate resin **10c**.

The individual components chosen for the 96-member library are shown in Figure 4. The components used to

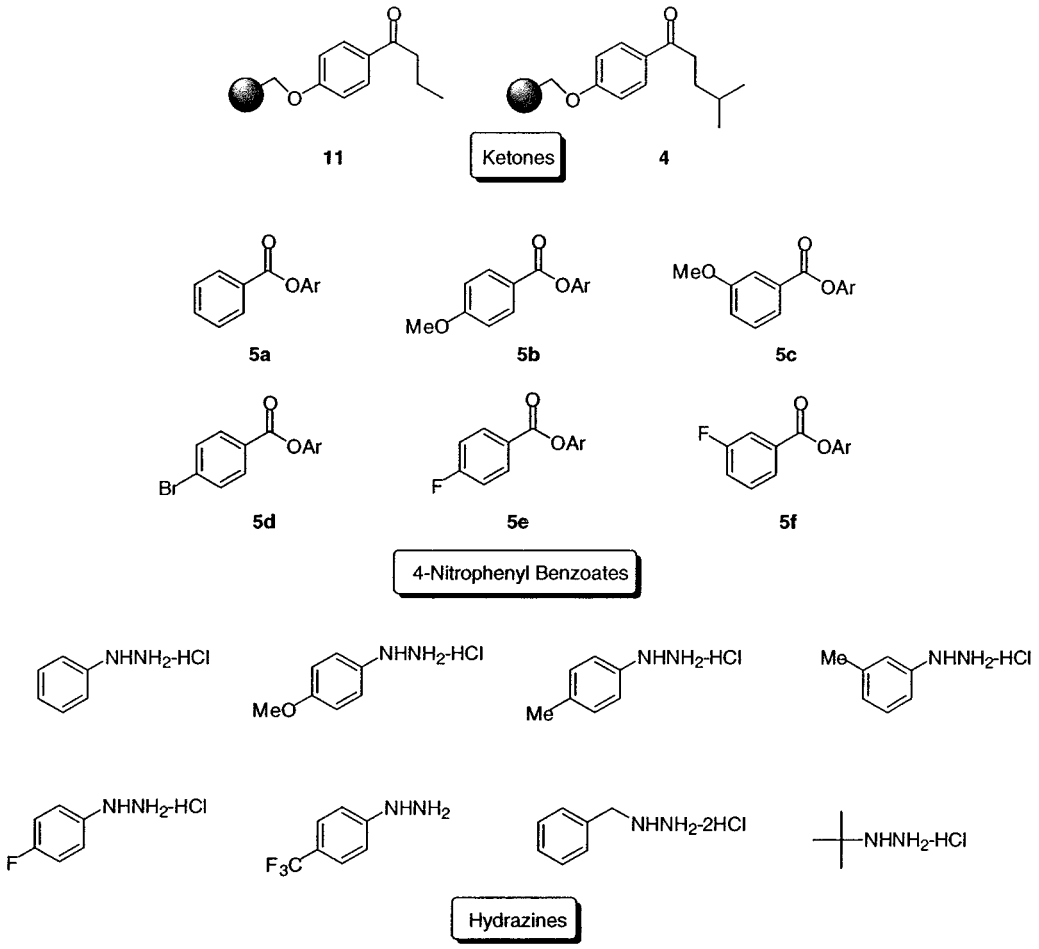

Figure 4. Components for 96-member pyrazole library.

Scheme 2. Development and Use of Bicarbonate Resin for HBr Neutralization

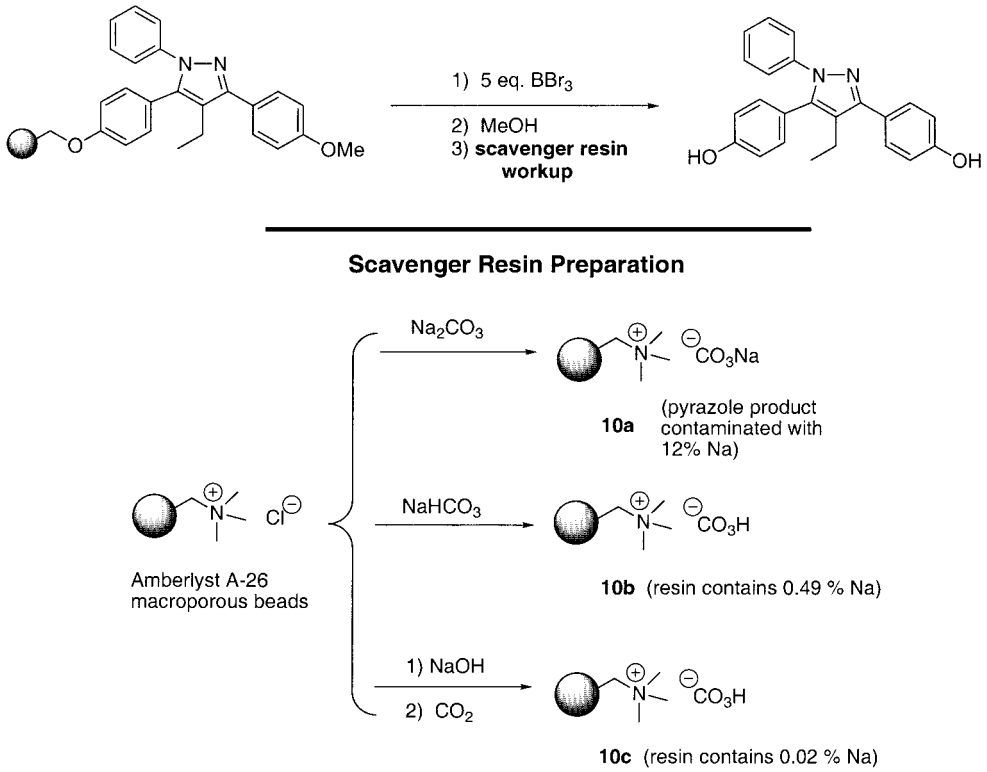

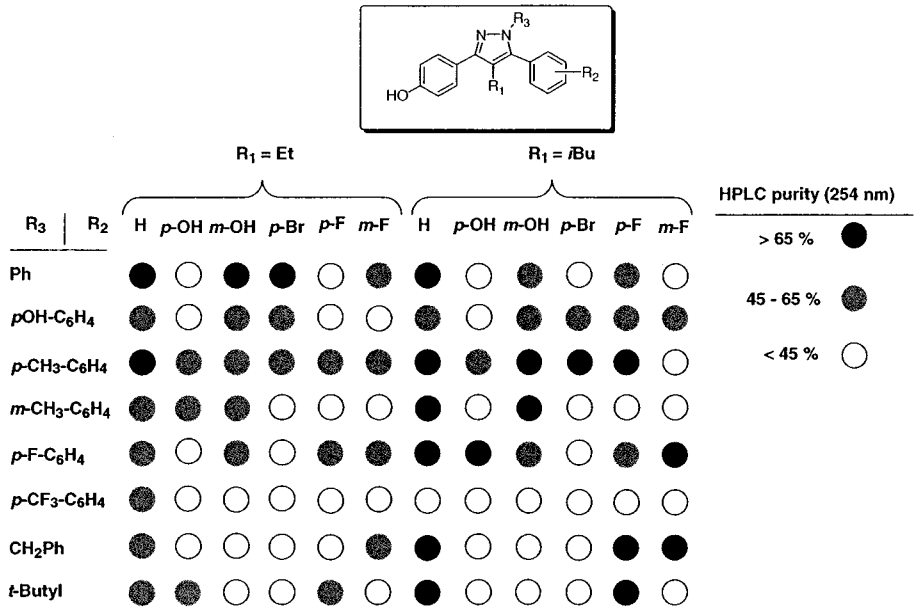

Figure 5. HPLC purities for 96-member ER library.

prepare the *i*-butyl library (Figure 2, Table 1) were again included as standards to measure the success and reproducibility of the synthesis and to verify the RBA assays. The progress of pyrazole formation for suspected "worst-case" combinations, such as CF_3-phenyl and *tert*-butyl hydrazines reacting with halogen-substituted diones, was monitored using FT-IR. The disappearance of the C═O signal at 1670 cm^{-1} was a reliable marker for determining the progress of individual reactions. Unfortunately, for several CF_3-substituted hydrazines we were unable to drive the reaction to completion, even after subjecting these resins to fresh reagent and heating for an additional 20 h. In any event, cleavage/deprotection with BBr_3 followed, and reactions were carefully quenched with MeOH and then incubated with bicarbonate resin **10c** for 1 h at 50−60 °C to ensure complete HBr neutralization and bromide ion sequestration. After being cooled, the pyrazole products were collected and concentrated, then reconstituted in 1 mL MeOH and analyzed using a standard, steep gradient elution on a high throughput reverse-phase HPLC column. Because the pyrazoles are uniformly fluorescent, we used fluorescence detection in tandem with UV detection to identify which of the eluted peaks was the pyrazole. This proved to be a robust approach to characterizing product purity. After obtaining the purity for each member, we determined the ER binding affinity in a simplified, three-point assay (see Experimental Section for details).

Purity and ER Binding Affinity Relationships. A summary of the HPLC purities for the final pyrazoles is shown in Figure 5, according to gray scale coded ranges. The average purity for the library was 50% (±15%). This is not an unreasonable level of purity when you consider that this library included components, such as *tert*-butyl hydrazine hydrochloride, which we have found to be less reactive than the aromatic hydrazines. As before, the principal impurities could be identified as the unreacted dione precursors, which we had previously shown did not affect the results of the binding assay (see above). On the basis of product yields, *p*-CF_3-substituted phenyl hydrazines appear to be even less reactive than *t*-butyl hydrazine hydrochloride, because this group of pyrazoles had the lowest overall purity of the whole library. Where regioisomers were expected within this series (see above), it was difficult to assign the product peaks, even with the help of fluorescence as a marker. In these cases, we assumed the purity to be 30%.

Shown in Figure 6 are the relative binding affinity (RBA) values for the 96-member library, indicated as ranges according to a gray scale coded legend. Several members of the library showed appreciable affinity for the ER. Particularly gratifying was the fact that most members of the 12-member *i*-butyl control library (Table 1) had RBA values which were reproduced quite well in the larger library (i.e., within 30%, relative), with the exception of **8f** (7.6%) vs **B-8** (23%). A repeat assay **8f** showed that its determination in the original 12-member library was low. The binding affinity of 16 additional select members was also re-tested after chromatographic purification (>80%), and the RBA values for these members also agreed quite well with the original determinations on the crude isolated products.

The use of an affinity array chart in Figure 6 permits a rapid, visual assessment of binding affinity patterns. For example, it is readily apparent that, for pyrazoles in both the R_1 ethyl and *i*-butyl series (column 2 and 8), those with HO substituents at R_2 have, overall, the highest affinity. Within these two series (columns 2 and 8), a number of substituents are tolerated at R_3, the best being *p*-HO−C_6H_4, for which the two highest affinity pyrazoles are represented, pyrazole **B-2** (14%) and **B-8** (23%). For pyrazoles with R_3 = *p*-HO−C_6H_4 (row B), a number of substituents are tolerated to varying degrees; those with fluorine substituents on R_2 for both the ethyl and *i*-butyl series bind moderately well (RBA = 1−5%). For members with R_1 = *i*-butyl and R_3 = *p*-HO−C_6H_4, even more polar substituents appear to bind well. Particularly noteworthy is the *m*-HO analogue **B-9**, which has a relative binding affinity of 6.8%, and the fluoro derivative **B-11**. By contrast, few other R_3 substituents are

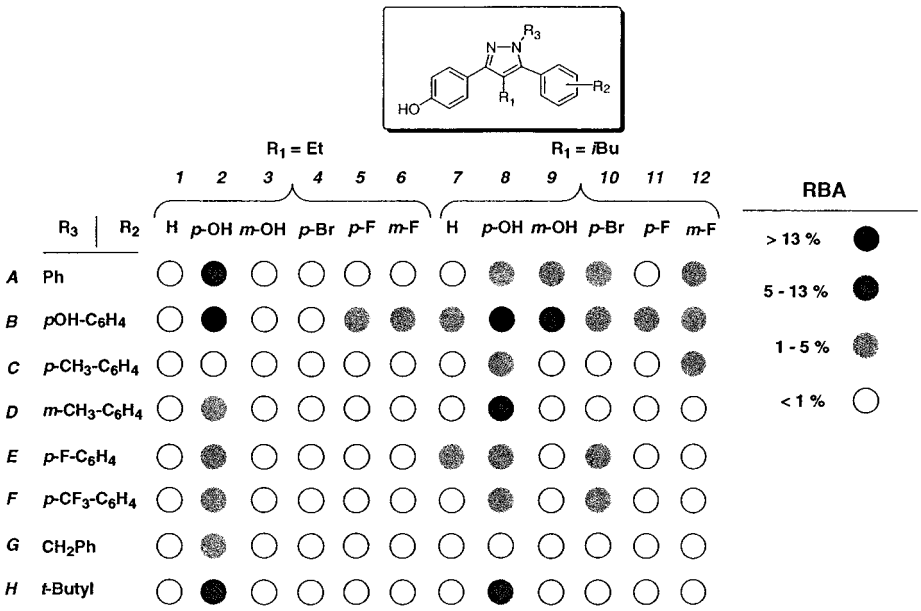

Figure 6. ER binding affinity for 96-member pyrazole library. (In unsymmetrical systems, i.e., $R_2 \neq$ *p*-OH, the average regioisomer ratio was 1.4 to 1.)

well tolerated by the ER, one exception, however, being the *tert*-butyl pyrazoles **H-2** and **H-8**, which each have affinities of 6−7%. As was the case with pyrazole **8j** from the 12-member *i*-butyl library, several pyrazoles with *p*-bromo substituents at R_2 have reasonable affinity (∼2−3%). However, these affinities are much lower when R_1 = ethyl (RBA <1%), than when R_1 = *i*-butyl.

In investigations to be reported elsewhere (Stauffer, S. R., Coletta, C. J., Sun, J., Katzenellenbogen, B. S., Katzenellenbogen, J. A., unpublished), we have made other analogues based on the high affinity 1,3,5-*p*-hydroxyphenyl-pyrazole template, and we have found a compound with an RBA of 30% that shows very high affinity and potency selectivity for ERα. We have also prepared other pyrazoles that act as ERα potency selective antagonists (Stauffer, S. R., Huang, Y., Aron, Z. D., Coletta, C. J., Sun, J., Katzenellenbogen, B. S., Katzenellenbogen, J. A., upublished).

Conclusions

We have developed a consistent and efficient method to prepare and isolate tetrasubstituted pyrazoles using a solid-phase strategy, and we have used this approach for the production of small, discrete libraries of estrogen receptor (ER) ligands. A combination of FT-IR and nanoprobe ^{1}H NMR-MAS allowed us to characterize intermediates leading up to the final pyrazole products directly on the bead. We also developed a scavenging resin to afford the cleaved/deprotected products free from inorganic contaminants. Using this approach, we prepared a 12-member test library, and then a more extensive 96-member library, and we determined product purity and ER binding affinity of all the library members. Several interesting binding affinity patterns emerged from these studies, and they have provided us with clear directions for further exploration of these tetrasubstituted pyrazoles, through which we have found a high affinity and high potency agonist with excellent selectivity for ERα and pyrazoles that selectivity *antagonize* ERα.

Experimental Methods

General. Melting points were determined on a capillary apparatus and are uncorrected. All reagents and solvents were obtained from Aldrich, Fisher, or Mallinckrodt. Tetrahydrofuran was freshly distilled from sodium/benzophenone. Dimethylformamide was vacuum distilled prior to use and was stored over 4 Å molecular sieves. Et_3N was stirred with phenylisocyanate, filtered, distilled, and stored over 4 Å molecular sieves. All reactions were performed under a dry N_2 atmosphere unless otherwise specified. Radial preparative-layer chromatography was performed on a Chromatotron instrument (Harrison Research, Inc., Palo Alto, CA) using EM Science silica gel Kieselgel 60 PF_{254} as adsorbent. Flash column chromatography[16] was performed using Woelm 32−63 μm silica gel packing. Resin bound ketone **11** was prepared according to procedure outlined in Scheme 1 from commercially available 4′-methoxybutyrophenone or from anisole and the acid chloride.

^{1}H and ^{13}C NMR spectra were recorded on 400 or 500 MHz spectrometers, using $CDCl_3$ or MeOD as solvent. Chemical shifts were reported as parts per million downfield from an internal tetramethylsilane standard ($\delta = 0.0$ for ^{1}H) or from solvent references. NMR coupling constants are reported in hertz. ^{13}C NMR data were determined using either the Attached Proton Test (APT) experiment or standard ^{13}C pulse settings. Low resolution electrospray mass spectrometry was performed using a VG Quattro (quadrupole-hexapole-quadrupole, QHQ) mass spectrometer system (Fisons Instruments, VG Analytical; Manchester, U.K.).

FT-IR Analysis and Nanoprobe ^{1}H NMR-MAS Spectra. FT-IR analysis was performed on an FTIR spectrometer, and absorption bands are reported in cm^{-1}. Infrared analysis was accomplished by placing approximately 1−2 mg of resin between two NaCl plates, swelling the beads in $CHCl_3$, and immediately recording an FT-IR spectrum. Solid-phase NMR spectra were obtained on a Varian 500 MHz wide-bore spectrometer using a nanoprobe. The polystyrene-bound

dione intermediates **12a**−**l** were characterized using 2 mg or less of resin in a pre-swollen $CDCl_3$ solution (nanotube, approximately 40 μL total volume). The sample was spun about the magic angle (54.7 °C) at 2.3−2.5 kHz, and four scans were collected for each ^{1}H experiment, using a pulse width of 15 μs and delay time of 4 ms. Tetramethylsilane was used as an internal reference.

Relative Binding Affinity Assay. Ligand binding affinities (RBAs) using lamb uterine cytosol as a receptor source were determined by a competitive radiometric binding assay. This assay is conducted in 96-well microtiter plates in a total volume of 70 μL, using ca. 1 nM of estrogen receptor binding equivalents, 10 nM [^{3}H]estradiol as tracer, and dextran-coated charcoal as an adsorbent for free ligand.[17] On the basis of interspecies comparison, lamb uterus is thought to contain predominantly estrogen receptor subtype α.[18,19] All incubations were done at 0 °C for 18−24 h. Binding affinities are expressed relative to estradiol (RBA = 100%) and are reproducible with a coefficient of variation of 0.3. RBA determinations for the 96-member library were performed using a three-point assay, at ligand concentrations of 10^{-4}, 10^{-6}, and 10^{-8} M and were corrected for individual purity level.

Chemical Syntheses. 4′-Methoxy-4-methyl-valerylophenone (2). To a stirred solution of $AlCl_3$ (6.4 g, 48 mmol) in 1,2-dichloroethane at 0 °C was added 4-methyl-valeryl chloride (5.3 g, 39.0 mmol) dropwise over approximately 10 min. The resulting solution was warmed to room temperature, stirred for 0.5 h, then re-cooled to 0 °C, and a 1,2-dichloroethane solution of anisole (5.1 mL, 46 mmol in 20 mL) was added dropwise. The reaction was stirred at room temperature for 9 h, then cooled to 0 °C, quenched with H_2O, and extracted with CH_2Cl_2. The organic layer was washed with saturated $NaHCO_3$ and brine, then dried over $MgSO_4$, and concentrated to afford product as a pale yellow oil (6.0 g, 75%): ^{1}H NMR ($CDCl_3$) δ 0.94 (d, 6H, J = 6.0), 1.60 (m, 3H, overlapping methine and β-CH_2), 2.90 (t, 2H, J = 6.8), 3.87 (s, 3H), 6.92 (d, 2H, J = 8.8), 7.90 (d, 2H, J = 8.8); ^{13}C NMR ($CDCl_3$) δ 22.6, 28.5, 33.9, 36.4, 55.2, 113.5, 130.2, 163.6, 198.7; MS (EI, 70 eV) m/z 206.1 (M^+). Anal. ($C_{13}H_{18}O_2$): C, 75.69; H, 8.80. Found: C, 75.63; H, 8.59.

4′-Hydroxy-4-methyl-valerylophenone (3). To a stirred solution of $AlCl_3$ (19.4 g, 145 mmol) in benzene (300 mL) at 0 °C was added a benzene solution (60 mL) of ketone **2** over 20 min. The reaction mixture was then brought to reflux for 2 h. After cooling to room temperature the mixture was poured over 400 mL of water, and then the organic layer washed with saturated $NaHCO_3$ and brine. The organic layer was then dried over $NaSO_4$ and concentrated to afford the phenolic product as a tan solid which was then used directly in the next step to functionalize Merrifield's resin (8.97 g, 96%): ^{1}H NMR ($CDCl_3$) δ 0.94 (d, 6H, J = 6.0) 1.27 (m, 3H, overlapping methine and β-CH_2), 2.90 (t, 2H, J = 8), 6.87 (d, 2H, J = 8.5), 7.91 (d, 2H, J = 9.0).

Alkylphenone Loading onto Merrifield Resin (4, 11). To a solution of the phenolic ketone (28.0 mmol, either **3** or 4′-hydroxy-butyrophenone) in DMF (144 mL) at 0 °C was added NaH as a 60% oil dispersion (1.05 g, 26.4 mmol). The reaction mixture was returned to room temperature; Merrifield resin (5.74 g, 1.39 mmol/g Novabiochem, Inc.) was added, and the reaction was heated to 55 °C for 22 h. The solution was then cooled to room temperature and quenched by addition of methanol (150 mL). The resin-bound product was then isolated via vacuum filtration and rinsed with methanol/DMF 1:1 (1 × 300 mL), DMF (3 × 350 mL), CH_2Cl_2 (3 × 350 mL), and methanol (3 × 350 mL). The resulting salmon-colored resin was then dried in vacuo for 18 h to afford >6 g of immobilized ketone. FT-IR analysis revealed the C=O stretch at 1670 cm^{-1}, which verified that the resin-bound ketone was produced. In addition, %Cl analysis was performed to verify the absence of halogen, indicating that most of the chloromethyl sites were substituted. Loading capacity, which ranged from 0.9 to 1.1 mmol/g, was determined from the mass recovery of expected product by cleaving a small portion of the ketone resin using BF_3−SMe_2.

General Procedure for Preparation of *p*-Nitrophenyl Benzoate Esters (5a−f). To a mechanically stirred solution of the substituted benzoic acid (52.6 mmol), *p*-nitrophenol (22.2 g, 157.8 mmol), and DMAP (3.2 g, 26.3 mmol) in 100 mL CH_2Cl_2 at 0 °C was added diisopropylcarbodiimide (57.9 mmol) dissolved in CH_2Cl_2 (100 mL) dropwise over 10 min. The resulting solution was allowed to stir for 18 h at room temperature. The reaction mixture was filtered, and the filtrate was concentrated under reduced pressure. The crude esters were recrystallized from EtOH or EtOAc to afford the desired ester (55−95%). Products were judged pure by comparison to literature melting points[20] and then used in the next step of the synthesis.

2-Ethyl-1,3-bis-(4-hydroxyphenyl)-propane-1,4-dione (9). The methoxy-protected derivative of **1** (prepared in 95% yield from 4-methoxybutyrophenone and the *p*-nitrophenyl-benzoate ester using LHMDS, under the same conditions used for the solid-phase synthesis; see **12a**−**l**, and purified by flash chromatography (ethyl acetate/hexanes)) was treated with 5 equiv of 1.0 M BBr_3 in CH_2Cl_2 at 0 °C. The mixture was allowed to reach room temperature and stir for 5 h. The reaction was then re-cooled to 0 °C and carefully quenched with water and repeatedly extracted with Et_2O. The combined organic layers were dried over Na_2SO_4, and upon solvent removal the title compound was afforded as a tan foam: ^{1}H NMR (MeOD) δ 0.99 (t, 3H, J = 7.5), 2.01 (q, 2H, J = 7.5) 5.32 (t, 1H, J = 1.5), 6.81 (AA′BB′, 2H, J = 7.0, 3.0), 7.90 (AA′BB′, 2H, J = 6.5, 3.0); ^{13}C NMR (MeOD) δ 11.4, 23.0, 56.6, 115.1, 128.0, 130.9, 162.8, 195.9; MS (EI, 70 eV) m/z 284 (M^+). Anal. ($C_{12}H_{16}O_4$): C, 71.28; H, 5.67. Found: C, 70.90; H, 5.57.

Preparation of Bicarbonate Form of Amberlyst A-26 Resin Using NaOH/CO_2 (10c). A medium sintered glass filter containing 15 g of Amberlyst A-26 resin in the chloride form (average capacity ~3.7 mequiv/g) was treated portionwise with 1 L of an aqueous 1.0 M NaOH solution. The resin in the hydroxide form was then dried under aspirator vacuum and suspended in a 150 mL water solution. A flow of CO_2 gas was bubbled into the aqueous solution for approximately 30 min with gentle mixing. The resin was then washed sequentially with MeOH, acetone, and ether,

and then extensively dried in vacuo. Elemental analysis indicated essentially no Na ion contamination (0.02%).

Solid-Phase Conditions Used To Prepare 12-Member Pyrazole Library (8a−l). A THF suspension for each of the six dione resins (50 mg, loading capacity 0.92−0.98 mmol/g, prepared according to procedure below), one of the four appropriate hydrazine hydrochlorides (15 equiv), and triethylamine (15 equiv) in toluene (2 mL) were heated to 80 °C for 9 h in a glass cell culture tube with a Teflon-lined screwed cap. Mixing was achieved using a rotating reaction block via a modified rotary evaporator motor. The reaction mixtures were cooled to room temperature and then isolated via vacuum filtration in coarse sintered glass frits. The product resins were rinsed with methanol/DMF 1:1 (2 × 5 mL), DMF (3 × 5 mL), CH_2Cl_2 (3 × 10 mL), and methanol (2 × 5 mL). The resulting resins were dried in vacuo for 18 h and then pre-swollen in a 2 mL CH_2Cl_2 solution under N_2 at −78 °C, using 10 mL conical vials, each containing a magnetic stir bar. Pyrazole cleavage/deprotection was followed by addition of 1 M BBr_3 (5 equiv, 0.7 mL) in CH_2Cl_2. The reaction was allowed to warm to room temperature and stir for 6 h and was quenched at 0 °C by the addition of CH_3OH (2 mL). The resins were isolated by vacuum filtration and rinsed twice with 5 mL portions of CH_3OH. The individual filtrates were concentrated in vacuo, dissolved in MeOH, and concentrated once again. This procedure was repeated twice, prior to RP-HPLC analysis. Pyrazoles **8a−l** were then purified to >80% HPLC purity by radial chromatography (10−20% MeOH/CH_2Cl_2) and submitted for ES-MS and RBA analysis. The expected molecular ion pattern by electrospray was observed in all cases: **(8a)** ES-MS calcd for $C_{25}H_{24}N_2$ 368.4, found MH^{2+} 370.1 (individual isomers separately measured); **(8b)** ES-MS calcd for $C_{25}H_{24}N_2O_2$ 384.5, found MH^+ 385.2 (individual isomers separately measured); **(8c)** ES-MS calcd for $C_{25}H_{23}FN_2O$ 386.5, found MH^+ 387.2; **(8d)** ES-MS calcd for $C_{23}H_{28}N_2O$ 348.5, found MH^+ 349.1; **(8e)** ES-MS cacld for $C_{25}H_{24}N_2O_2$ 384.5, found MH^{2+} 386.2; **(8f)** ES-MS calcd for $C_{25}H_{24}N_2O_3$ 400.5, found MH^+ 401.1; **(8g)** ES-MS calcd for $C_{25}H_{23}FN_2O_2$ 402.5, found MH^+ 403.1; **(8h)** ES-MS calcd for $C_{23}H_{28}N_2O_2$ 364.5, found MH^+ 365.2; **(8i)** ES-MS calcd for $C_{25}H_{23}BrN_2O$ 446.1, found MH^+ 447.0 (individual isomers separately measured); **(8j)** ES-MS calcd for $C_{25}H_{23}BrN_2O_2$ 462.1, found MH^+ 463.1; **(8k)** ES-MS calcd for $C_{25}H_{22}BrFN_2O$ 464.1, found MH^+ 465.1; **(8l)** ES-MS calcd for $C_{23}H_{27}BrN_2O$ 426.1, found MH^+ 427.2.

General Procedure for Batch Dione Synthesis (12a−l). Twelve conical polypropylene cell culture tubes (20 mL) were charged with 400 mg of ketone resin (**4** and **11**, approximately 0.38 mmol, six tubes per ketone), *p*-nitrophenyl esters (5.76 mmol, **5a−c**), and 15 mL of THF. Each tube was then purged with a nitrogen atmosphere using a 14/20 septa and then chilled in an ice bath. A 1.0 M THF solution of LHMDS (3.84 mmol) was added dropwise via syringe to each tube; the reaction was then sealed with a screw cap and shaken vigorously. Esters **5d−f** could not be present during enolate formation due to their reactivity toward LHMDS and thus were added in one portion 30 min after addition of LHMDS. All 12 reaction tubes were then loaded into a homemade reaction block, which was slowly rotated within a 40 °C oven using a modified rotary evaporator motor. After 5 h, the resins were transferred to coarse sintered glass filters using CH_2Cl_2. A rinse procedure followed involving methanol/DMF 1:1 (1 × 30 mL), DMF (3 × 20 mL), CH_2Cl_2 (3 × 20 mL), and methanol (2 × 20 mL). The resins were then dried in vacuo, and the level of product formation was determined by nanoprobe ^1H NMR-MAS. In all 12 cases, disappearance of the ketone α-protons occurred, and a new signal at approximately δ 5−5.3 was observed for the α/α′ methine proton, indicating successful dione formation. Diagnostic chemical shifts are reported below (note: aromatic resonances from dione which overlap with polystyrene backbone in addition to the resin backbone signals themselves are not listed; for purposes of naming, polystyrene is abbreviated "PS"; integration values are approximately ±15%).

1-PS-(4-Benzyloxyphenyl)-2-ethyl-3-phenyl-propane-1,3-dione (12a): δ 1.02 (3H, C*H*$_3$CH$_2$), 2.15 (2H, CH$_3$C*H*$_2$), 4.95 and 5.05 (two overlapping s, 3H, PS-ArC*H*$_2$O and α/α′-C*H*), 7.95 (4H, ArC*H ortho*-C═O).

1-PS-(4-Benzyloxyphenyl)-2-ethyl-3-(4-methoxyphenyl)-propane-1,3-dione (12b): δ 1.01 (3H, C*H*$_3$CH$_2$), 2.15 (2H, CH$_3$C*H*$_2$), 3.74 (3H, OC*H*$_3$), 4.98 (s, 3H, ArC*H*$_2$ and α/α′-C*H*), 7.95 (4H, ArC*H ortho*-C═O).

1-PS-(4-Benzyloxyphenyl)-2-ethyl-3-(3-methoxyphenyl)-propane-1,3-dione (12c): δ 1.02 (3H, C*H*$_3$CH$_2$), 2.14 (2H, CH$_3$C*H*$_2$), 3.72 (3H, OC*H*$_3$), 5.05 (two overlapping s, 3H, PS-ArC*H*$_2$O and α/α′-C*H*), 7.51 (2H, ArC*H*), 7.96 (2H, ArC*H*).

1-PS-(4-Benzyloxyphenyl)-2-ethyl-3-(4-bromophenyl)-propane-1,3-dione (12d): δ 1.01 (3H, C*H*$_3$CH$_2$), 2.13 (2H, CH$_3$C*H*$_2$), 4.97 (s, PS-ArC*H*$_2$O and α/α′-C*H*); 7.50 (ArC*H*), 7.79 (ArC*H*), 7.95 (ArC*H*).

1-PS-(4-Benzyloxyphenyl)-2-ethyl-3-(4-fluorophenyl)-propane-1,3-dione (12e): δ 1.01 (3H, C*H*$_3$CH$_2$), 2.14 (2H, CH$_3$C*H*$_2$), 4.97 (s, PS-ArC*H*$_2$O and α/α′-C*H*), 7.97 (4H, ArC*H*).

1-PS-(4-Benzyloxyphenyl)-2-ethyl-3-(3-fluorophenyl)-propane-1,3-dione (12f): δ 1.01 (3H, C*H*$_3$CH$_2$), 2.13 (2H, CH$_3$C*H*$_2$), 4.97 (s, PS-ArC*H*$_2$O and α/α′-C*H*), 7.64, 7.69, 7.95 (three s, 4H, ArC*H*).

1-PS-(4-Benzyloxyphenyl)-2-*iso*-butyl-3-phenyl-propane-1,3-dione (12g): δ 0.96 (6H, (C*H*$_3$)$_2$), 2.01 (β-C*H*$_2$), 4.95 (2H, PS-ArC*H*$_2$O), 5.24 (1H, α/α′-C*H*), 7.39 (3H, ArC*H*), 7.48 (ArC*H*), 7.97 (3H, ArC*H*).

1-PS-(4-Benzyloxyphenyl)-2-*iso*-butyl-3-(4-methoxyphenyl)-propane-1,3-dione (12h): δ 0.95 (6H, (C*H*$_3$)2), 2.02 (β-C*H*$_2$), 3.76 (3H, OC*H*$_3$), 4.93 (2H, PS-ArC*H*$_2$O), 5.17 (1H, α/α′-C*H*), 7.97 (4H, ArC*H*).

1-PS-(4-Benzyloxyphenyl)-2-*iso*-butyl-3-(3-methoxyphenyl)-propane-1,3-dione (12i): δ 0.96 (6H, (C*H*$_3$)$_2$), 2.00 (β-C*H*$_2$), 3.74 (3H, OC*H*$_3$), 4.95 (2H, PS-ArC*H*$_2$O), 5.23 (1H, α/α′-C*H*), 7.29 (ArC*H*), 7.52 (2H, ArC*H*), 7.97 (2H, ArC*H*).

1-PS-(4-Benzyloxyphenyl)-2-*iso*-butyl-3-(4-bromophenyl)-propane-1,3-dione (12j): δ 0.95 (6H, (C*H*$_3$)$_2$), 1.97 and 2.05 (overlapping s, β-C*H*$_2$), 4.95 (2H, PS-ArC*H*$_2$O), 5.14 (1H, α/α′-C*H*), 7.51 (2H, ArC*H*), 7.81 (2H, ArC*H*), 7.96 (3H, ArC*H*).

1-PS-(4-Benzyloxyphenyl)-2-*iso*-butyl-3-(4-fluorophenyl)-propane-1,3-dione (12k): δ 0.95 (6H, (CH_3)$_2$), 1.99 and 2.05 (overlapping s, β-CH_2), 4.95 (2H, PS-ArCH_2O), 5.16 (1H, α/α'-C*H*), 7.98 (4H, ArC*H*).

1-PS-(4-Benzyloxyphenyl)-2-*iso*-butyl-3-(3-fluorophenyl)-propane-1,3-dione (12l): δ 0.95 (6H, (CH_3)$_2$), 1.95 and 2.07 (overlapping s, β-CH_2), 4.97 (2H, PS-ArCH_2O), 5.18 (1H, α/α'-C*H*), 7.66 (ArC*H*), 7.73 (ArC*H*), 7.97 (4H, ArC*H*).

General Solid-Phase Conditions Used To Prepare 96-Member Pyrazole Library. Pyrazole Formation: Each of the above diones (**12a**−**l**) were divided into eight approximately 50 mg portions and distributed across each row of an 8 × 12 Polyfiltronics Unifilter plate. After charging each well with the appropriate dione, the 12 commercially available hydrazine components (Figure 4) were carefully added as preweighed solids to the appropriate wells while carefully blocking off neighboring wells in order to avoid cross-contamination. The bottom of the plate was then secured in a reaction clamp (Polyfiltronics Combiclamp) with two Viton gaskets. To each well was added 1.5 mL of EtOH and approximately 100 μL of TEA. The top of the plate was sealed and the assembly agitated and heated to 65 °C in an oscillating cell culture oven. The reaction was monitored by FT-IR using several suspected "worst-case" scenarios (**H-2**, **F-2**, and **E-5** and our lead compound, **A-2**) by observing the diminishing intensity of the C═O signal at 1670 cm^{-1}. After 38 h, the plate was cooled to room temperature, and the crude mixtures were filtered within the reaction block by vacuum aspiration (Polyfiltronics filter/collection vacuum manifold). The resin-bound pyrazoles were then rinsed with methanol/DMF 1:1 (2 × 2 mL), DMF (3 × 2 mL), CH_2Cl_2 (3 × 2 mL), and methanol (3 × 2 mL) and then dried in vacuo overnight in a desiccator.

Deprotection/Cleavage: In a N_2-charged glovebag at room temperature, the resins were suspended in 0.5 mL of CH_2Cl_2 and treated dropwise with a 1.0 M CH_2Cl_2 solution of BBr_3 (500 μL). The reaction block was sealed as before and allowed to stand at room temperature with occasional mixing. After 8 h, the resins were carefully quenched with cold MeOH (0.5 mL), and then approximately 100 mg of bicarbonate resin **10c** was added to each well. After 20 min, when most of the CO_2 evolution ceased, the reaction top was resealed and the block heated to 50−60 °C for 1 h. Upon cooling to room temperature, the released library members were collected in a 96-well 2 mL collection plate, and the solvent evaporated to dryness (a 96-pin manifold capable of providing a gentle overhead stream of N_2 to each well in addition to gentle warming using a hot plate allowed for the removal of most of the MeOH; the remaining residual volatiles were removed in vacuo). Each member was then reconstituted in 1 mL of MeOH and analyzed by RP-HPLC.

Characterization of 96-Member Pyrazole Library. RP-HPLC analysis was performed on an analytical HPLC system with an autosampler. UV detection was performed at 254 nm and a flow rate of 1.0 mL/min using a C-18 CombiScreen analytical column (YMC, Inc., 4.6 mm × 50 mm) with a MeOH:H_2O gradient solvent system (40−90% MeOH, 0−5 min, total run time = 10 min). A fluorometer HPLC flow detector was used to aid in identification of the expected pyrazole peak. An excitation wavelength of 306 nm and emission wavelength of 364 nm were used, based on the fluorescence properties of pyrazole **1**. After RP-HPLC analysis, the library members were transferred from autosampler vials to tared 7 × 40 mm flat bottom vials (8 mm crimp tops), and the solvent was then removed using a Savant vacuum centrifuge. After further drying in vacuo the sample weight was recorded, and a modified three-point competitive binding assay was then performed. Authentic HPLC traces obtained for **8a**−**l** (Table 1) were used to help confirm their later synthesis in the 96-member library. These controls represent 13% of the total library members produced. The RBA values of these "controls" from this library were equivalent to those obtained for the same compounds in the 12-membered library, within the statistical limits of the binding assay (coefficient of variation is 0.3).

Acknowledgment. We are grateful for support of this research through grants from the U.S. Army Breast Cancer Research Program (DAMD17-97-1-7076) and the National Institute of Health (HHS 5R37 DK1556). We thank Kathryn E. Carlson for performing binding assays. NMR spectra were obtained in the Varian Oxford Instrument Center for Excellence in NMR Laboratory. Funding for this instrumentation was provided in part from the W. M. Keck Foundation and the National Science Foundation (NSF CHE 96-10502). Mass spectra were obtained on instruments supported by grants from the National Institute of General Medical Sciences (GM 27029), the National Institute of Health (RR 01575), and the National Science Foundation (PCM 8121494).

References and Notes

(1) Dolle, R. E.; Nelson, K. H. J. Comprehensive Survey of Combinatorial Library Synthesis. *J. Comb. Chem.* **1999**, *1*, 235−282.
(2) Grese, T. A.; Dodge, J. A. Selective Estrogen Receptor Modulators (SERMS) [Review]. *Curr. Pharm. Des.* **1998**, *4*, 71−92.
(3) Grese, T. A.; Sluka, J. P.; Bryant, H. U.; Cullinan, G. J.; Glasebrook, A. L.; Jones, C. D.; Matsumoto, K.; Palkowitz, A. D.; Sato, M.; Termine, J. D.; Winter, M. A.; Yang, N. N.; Dodge, J. A. Molecular determinants of tissue selectivity in estrogen receptor modulators. *Proc. Natl. Acad. Sci. U.S.A.* **1997**, *94*, 14105−14110.
(4) Willard, R.; Jammalamadaka, V.; Zava, D.; Benz, C. C.; Hunt, C. A.; Kushner, P. J.; Scanlan, T. S. Screening and characterization of estrogenic activity from hydroxystilbene library. *Chem. Biol.* **1995**, *2*, 45−51.
(5) Brown, D. S.; Armstrong, R. W. Synthesis of tetrasubstituted ethylenes on solid support via resin capture. *J. Am. Chem. Soc.* **1996**, *118*, 6331−6332.
(6) Fink, B. E.; Mortensen, D. S.; Stauffer, S. R.; Aron, Z. D.; Katzenellenbogen, J. A. Novel structural templates for estrogen-receptor ligands and prospects for combinatorial synthesis of estrogens. *Chem. Biol.* **1999**, *6*, 205−219.
(7) Sun, J.; Meyers, M. J.; Fink, B. E.; Rajendran, R.; Katzenellenbogen, J. A.; Katzenellenbogen, B. S. Novel ligands that function as selective estrogens or antiestrogens for estrogen receptor-α or estrogen receptor-β. *Endocrinology* **1999**, *140*, 800−804.
(8) Nilsson, S.; Kuiper, G.; Gustafsson, J. A. ER beta: a novel estrogen receptor offers the potential for new drug development [Review]. *Trends Endocrinol. Metab.* **1998**, *9*, 387−395.
(9) Marzinik, A. L.; Felder, E. R. Solid support synthesis of highly functionalized pyrazoles and isoxazoles; scaffolds for molecular diversity. *Tetrahedron Lett.* **1996**, *37*, 1003−1006.
(10) Marzinzik, A. L.; Felder, E. R. Key intermediates in combinatorial chemistry: access to various heterocycles from α,β-unsaturated ketones on the solid phase. *J. Org. Chem.* **1998**, *63*, 723−727.

(11) Watson, S. P.; Wilson, R. D.; Judd, D. B.; Richards, S. A. Solid-phase synthesis of 5-aminopyrazoles and derivatives. *Tetrahedron Lett.* **1997**, *38*, 9065−9068.
(12) Wilson, R. D.; Watson, S. P.; Richards, S. A. Solid-phase synthesis of 5-aminopyrazoles and derivatives. *Tetrahedron Lett.* **1998**, *39*, 2827−2830.
(13) Green, J. Solid-Phase synthesis of lavendustin analogues. *J. Org. Chem.* **1995**, *60*, 4287−4290.
(14) Boojamra, C. G.; Burow, K. M.; Ellman, J. A. An Expedient and High-Yielding Method for the Solid-Phase Synthesis of Diverse 1,4-Benzodiazepine-2,5-Diones. *J. Org. Chem.* **1995**, *60*, 5742−5743.
(15) Cardillo, G.; Orena, M.; Porzi, G.; Sandri, S. Carbonate ion on a polymeric support: hydrolysis of alkyl halides and cyclic iodocarbonates. *Synthesis* **1981**, 793−794.
(16) Still, W. C.; Kahn, M.; Mitra, A. Rapid chromatographic technique for preparative separations with moderate resolution. *J. Org. Chem.* **1978**, *43*, 2923−2926.
(17) Katzenellenbogen, J. A.; Johnson, H. J., Jr.; Myers, H. N. Photoaffinity labels for estrogen binding proteins of rat uterus. *Biochemistry* **1973**, *12*, 4085−4092.
(18) Kuiper, G. G. J. M.; Carlsson, B.; Grandien, K.; Enmark, E.; Häggblad, J.; Nilsson, S.; Gustafsson, J.-Å. Comparison of the ligand binding specificity and transcript tissue distribution of estrogen receptor α and *β*. *Endocrinology* **1997**, *138*, 863−870.
(19) Mosselman, S.; Polman, J.; Dijkema, R. ER*β*: identification and characterization of a novel human estrogen receptor. *FEBS* **1996**, *392*, 49−53.
(20) O'Connor, C. J.; Lomax, T. D. The reactivity of *p*-nitrophenyl esters with surfactants in apolar solvents. VII* substituent effects on the reactivity of 4′-nitrophenyl 4-substituted benzoates in benzene solutions of dodecylammonium propionate and butane-1,4-diamine bis(dodecanoate). *Aust. J. Chem.* **1983**, *36*, 917−925.

CC0000040